Velocity lag between particle and liquid in sediment-laden open channel turbulent flow

Article *in* European Journal of Mechanics - B/Fluids · November 2015

Impact Factor: 1.66 · DOI: 10.1016/j.euromechflu.2015.11.003

3 authors, including:

Debasish Pal

Singapore University of Technology and De…

10 PUBLICATIONS **14** CITATIONS

European Journal of Mechanics B/Fluids 56 (2016) 130–142

Contents lists available at ScienceDirect

European Journal of Mechanics B/Fluids

journal homepage: www.elsevier.com/locate/ejmflu

Velocity lag between particle and liquid in sediment-laden open channel turbulent flow

Debasish Pal [a,*], Sanjeev Kumar Jha [b], Koeli Ghoshal [a]

[a] Department of Mathematics, Indian Institute of Technology Kharagpur, Kharagpur 721302, India
[b] School of Civil and Environmental Engineering, University of New South Wales, Sydney 2052, Australia

HIGHLIGHTS

- Model on velocity lag between liquid and particle in open channel flow is derived.
- Hindered drag force and impact, viscous and turbulent shear stresses are included.
- Effects of particle–particle and particle–liquid interactions are considered.
- The suggested model is validated with a wide range of existing experimental data.
- The proposed model provides better result in comparison to other existing models.

ARTICLE INFO

Article history:
Received 6 July 2015
Received in revised form
7 October 2015
Accepted 11 November 2015
Available online 30 November 2015

Keywords:
Velocity lag
Open channel
Turbulent flow
Particle–liquid interaction
Particle–particle interaction
Random dispersion

ABSTRACT

This study focuses on the prediction of velocity lag between particle and liquid in sediment-laden open channel turbulent flow. From theoretical point of view, we formulate a mathematical model of velocity lag based on hindered drag force on particle, impact shear stress, viscous shear stress and turbulent shear stress which are derived from the viewpoint of turbulence, particle–liquid interaction, particle–particle interaction and random dispersion of suspended sediment owing to these interactions. No estimation of empirical parameter is required for calculating velocity lag from the resultant model. The profile of velocity lag obtained is a function of particle diameter, mass density of sediment particle, shear velocity and vertical height from channel bed. The model also explains real phenomenological characteristics of velocity lag caused by the interaction between particle and liquid during turbulent flow. Our model well agrees with a wide range of twenty-two experimental runs collected from published literature. In addition, error analysis proves the superior prediction accuracy of our model in comparison to other existing models of velocity lag.

1. Introduction

Understanding the interaction between particle and liquid in sediment-laden open channel turbulent flow is one of the key issues in river geomorphological studies due to its impact on erosion and sedimentation. Traditional approaches did not take into account the complex mechanism involved in sediment transport and the two phases of particle and liquid are assumed as a sediment–liquid mixture during transportation [1–4]. By the advent of several advanced measurement techniques such as phase-Doppler anemometry (PDA), particle image velocimetry (PIV), particle tracking velocimetry (PTV), laser-Doppler anemometry (LDA), and discriminator laser-Doppler velocimetry (DLDV), separate measurement of particle and liquid velocities in sediment-laden flow has become possible and this advantage helps to understand the lag between particle and liquid phases for different turbulent features. Several experiments [5–14] have been done to predict the effect of different flow parameters on the lag of various turbulent quantities between liquid and particle phases. These experimental investigations reveal the velocity difference between particle and liquid phases and this difference contradicts the previous assumption [1–4] that sediment-laden flow can be considered as a simple mixture of particle and liquid.

Besides these experimental studies, literature [15–17] were based on the two-phase flow theory also discuss about velocity lag. Depending upon the concentration level of particles and

* Corresponding author.
E-mail address: bestdebasish@gmail.com (D. Pal).

http://dx.doi.org/10.1016/j.euromechflu.2015.11.003
0997-7546/

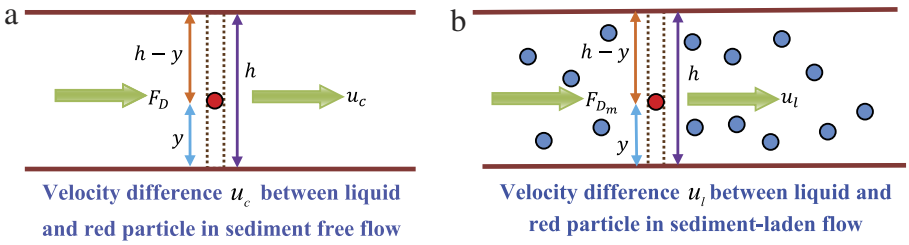

Fig. 1. Schematic diagram of (a) u_c and (b) u_l in flow region.

other physical properties in the flow, the governing equations of two-phase flow approach include one-way to four-way couplings which play significant role in the definition of particle's velocity [18,19]. Bombardelli and Jha [16] proposed hierarchy of two-phase flow models namely mixture model, partial two-phase flow model (PTFM) and complete two-phase flow model (CTFM) with increasing level of complexity in representing the flow through a set of equations. As the name indicates, implement of PTFM was made easier than CTFM by using the governing equations for mixture flow as surrogate for the fluid phase, thus reducing the complexity in numerical solution for solving mass and momentum equations of both phases. Our motivation for the present study stems from the fact that an analytical expression of streamwise velocity difference or velocity lag between liquid and particle in particle-laden flow would definitely reduce the complexity of PTFM by removing the need to calculate the velocity of particle.

Starting with two-phase flow theory, researchers analytically [20,21] or numerically [15] computed velocity lag and verified with limited experimental runs from published literature [5,8,12]. Chauchat and Guillou [15] did not consider the interparticle collision and frictional effects of wall, though they mentioned the significance of these turbulent features in predicting velocity lag. It is worth mentioning that the calculation of velocity lag through two-phase flow approach encounters difficulty in rigorous numerical solution subjected to the estimation of various empirical parameters. Besides the two-phase flow theory, Cheng [22] predicted a mathematical model of velocity lag based on a hindered drag force in sediment-laden flow and stated that the model has limitations when particles receive intensive boundary collisions near the channel bed and significant gradients of velocity and concentration exist in the flow.

From the aforementioned discussions, we can infer that a generalized model of velocity lag in dilute and non-dilute sediment-laden flows can be developed by modifying the drag force together with the inclusion of interactive forces in suspension region during flow. This study endeavors to propose an analytical model of velocity lag which might be helpful to overcome the rigorous numerical calculation of velocity lag from two-phase flow approach. We organize the paper as follows. Section 2 describes the formulation of velocity lag model based on hindered drag force on particle in sediment-laden flow, impact shear stress, viscous shear stress and turbulent shear stress which take into account the effects of turbulence, particle–liquid interaction, particle–particle interaction and random dispersive nature of suspended sediment due to these interactions. Section 3 explains the selection of a wide range of experimental data to verify our model. Section 4 delineates the assessment of our model in predicting velocity lag. Through graphical representations and an error analysis, Section 5 presents a detailed comparative analysis between experimental data, our model and other published velocity lag models. Section 6 provides detailed discussions on the rationalization of real phenomena of velocity lag by our model and its excellency in comparison to other models from several aspects. The paper ends with brief conclusion.

2. Mathematical modeling

We start the mathematical modeling in deriving a hindered drag force acting on a suspended particle in sediment-laden open channel turbulent flow. Next, we derive the other forces acting on that particle due to the surrounding liquid and the intimate presence of other suspended particles. Based on these expressions of forces, we propose our velocity lag model.

In particle-free flow, the driving drag force F_D acting on a single suspended particle is expressed as

$$F_D = C_D \frac{\pi D^2}{4} \frac{\rho_f u_c^2}{2} \tag{1}$$

where u_c is the relative velocity or velocity difference between particle and liquid along streamwise direction, C_D is the drag coefficient, D is the particle diameter and ρ_f is the mass density of liquid. Keeping the same fluid flux for F_D and the drag force F_{D_m} in the presence of other particles in sediment-laden flow, Di Felice [23] connected them by a hindrance function H as

$$F_{D_m} = HF_D \tag{2}$$

Following Cheng [22], we write F_{D_m} by

$$F_{D_m} = C_{D_m} \frac{\pi D^2}{4} \frac{\rho_m {u_l}^2}{2} \tag{3}$$

where u_l is the streamwise relative velocity or velocity difference between particle and liquid in sediment-laden flow, C_{D_m} is the drag coefficient in that flow and ρ_m is the mass density of sediment–liquid mixture. The velocity differences u_c and u_l are shown by schematic diagrams in Fig. 1(a) and (b) respectively. We write H from Eqs. (1)–(3) as

$$H = \frac{C_{D_m}}{C_D} \frac{\rho_m}{\rho_f} \frac{u_l^2}{u_c^2}. \tag{4}$$

By assuming the particle distribution to be locally uniform in a prismatic volume of liquid containing randomly distributed particles and replacing the local concentration of particles by the volumetric particles' concentration c, Cheng [22] proposed a relation between u_l and u_c by

$$u_l = \frac{u_c}{1-c}. \tag{5}$$

The drag coefficient C_D generally depends on the particle Reynolds number Re given by

$$\mathrm{Re} = \frac{u_c D}{\nu_f} \tag{6}$$

where ν_f is the kinematic viscosity of clear liquid. It is observed that irrespective of flow nature, C_D satisfies two asymptotic relations which are $C_D = A_1/\mathrm{Re}$ for $\mathrm{Re} < 1$ and $C_D = A_2$ for $\mathrm{Re} > 10^5$ where A_1 and A_2 are constants. From these characteristics, Cheng [24] suggested C_D for the intermediate range of Re by

$$C_D = \left[\left(\frac{A_1}{\mathrm{Re}} \right)^{\frac{1}{n}} + A_2^{\frac{1}{n}} \right]^n \tag{7}$$

where n is a constant. Through best fitting technique, Cheng [22] estimated the values of A_1, A_2 and n as 32, 1 and 1.5 respectively by matching Eq. (7) with experimental data of C_D for a broad range of Re($10^{-4} \leq$ Re $\leq 10^4$). For observing good agreement between Eq. (7) and experimental data, we refer the corresponding figure (Fig. 7) in the article of Cheng [22]. Therefore, these expressions of Re and C_D are considered in this study and we can express R_m and C_{D_m} for particle-laden flow in analogous to Eqs. (6) and (7) respectively as

$$R_m = \frac{u_l D}{\nu_m} \tag{8}$$

$$C_{D_m} = \left[\left(\frac{A_1}{R_m}\right)^{\frac{1}{n}} + A_2^{\frac{1}{n}}\right]^n \tag{9}$$

where ν_m is the kinematic viscosity of sediment–liquid mixture. To calculate H from Eq. (4), we need an expression of ρ_m. Generally, the mass density of each element in a mixture is multiplied by the concentration of that element in mixture and the summation of all these multiplications is considered as ρ_m. To the best of our knowledge, a theoretical or experimental proof in support of this phenomenon is unknown. Pal and Ghoshal [25] took into account the random dispersion of suspended particle owing to their interactions with surrounding liquid and other particles in suspension, and proposed ρ_m by

$$\rho_m = \rho_f (1-c)^{-\Delta_p} \tag{10}$$

where $\Delta_p = (\rho_p - \rho_f)/\rho_f$ in which ρ_p is the mass density of particle. The justification of this formula of ρ_m is given at the commencement of Section 3. Using Eqs. (5)–(10), the expression of hindrance function H given by Eq. (4) takes the form

$$H = (1-c)^{-(\Delta_p+2)}\left[\mu_r^{\frac{1}{n}}(1-c)^{\frac{1+\Delta_p}{n}} + \left(\mathrm{Re}\frac{A_2}{A_1}\right)^{\frac{1}{n}}\right]^n \times \left[1 + \left(\mathrm{Re}\frac{A_2}{A_1}\right)^{\frac{1}{n}}\right]^{-n} \tag{11}$$

where $\mu_r (= \mu_m/\mu_f)$ in which μ_f and μ_m are the dynamic viscosities of particle-free liquid and particle-laden liquid respectively. The formula of μ_m selected in this study is given at Appendix A.

After the derivation of H given by Eq. (11), our objective is to propose a generalized mathematical expression of u_l for dilute and non-dilute sediment-laden flow. To achieve this goal, a clear idea is required on the forces acting on a suspended particle enclosed by surrounding liquid and other neighboring particles in suspension. The nature of high concentration is ubiquitous near the channel bed irrespective of all open channel turbulent flow though its worth mentioning that a large number of suspended particles at far from the channel bed can be noticed for non-dilute sediment-laden flow. This high concentration generates impact shear stress τ_i due to particle–particle interaction and viscous shear stress τ_ν owing to the viscous interaction between suspended particles and their surrounding liquid. Apart from τ_i and τ_ν, the turbulent shear stress τ_f plays a significant role throughout the suspension region. For taking into account the effect of high concentration in τ_f, we consider it for the interstitial fluid of suspended particles. We derive the total shear stress for dilute and non-dilute sediment-laden flows as a summation of these mentioned shear stresses considered in terms of turbulence, particle–particle interaction, particle–liquid interaction and random dispersion of suspended sediment owing to these interactions.

Based on collisions between suspended sediment particles, Bagnold [26] investigated τ_i and his widely cited expression is given as

$$\tau_i \propto \rho_p \left(\frac{D^2}{G_a}\right)^2 \left(\frac{\partial u}{\partial y}\right)^2 \tag{12}$$

where u is the streamwise velocity of liquid in sediment-laden flow uniform along streamwise direction, y is the vertical height from channel bed and G_a is the average space between two randomly moving adjacent sediment particles in suspension. By considering the viscous interaction mechanism between suspended particle and their surrounding liquid, Ghoshal and Pal [27] proposed τ_ν by

$$\tau_\nu \propto \mu_m \frac{D^2}{D_m^2}\frac{D_m}{G_a}\frac{\partial u}{\partial y} \tag{13}$$

where D_m is the average distance between the centers of two randomly moving adjacent suspended particles. We consider the turbulent shear stress τ_f in the interstitial fluid of sediment particles for our research and therefore we select the expression proposed by Mih [28]. It is given as

$$\tau_f = -\rho_f \overline{u'v'}\frac{G_a}{D_m} \tag{14}$$

where u' and v' are the velocity fluctuations of liquid in sediment-laden flow along streamwise direction and perpendicular to streamwise direction respectively. By analyzing experimental data of sediment-laden flow from published literature [8,12,29], Kundu and Ghoshal [30] expressed $-\overline{u'v'}$ as

$$-\overline{u'v'} = u_*^2(1-\xi) \tag{15}$$

where u_* is the shear velocity and $\xi (= y/h)$ is the normalized vertical height from channel bed in which h is the flow depth. Following the concept of Mih [31] for granular flow, we write total shear stress τ_t as proportional to the summation of τ_i, τ_ν and τ_f; as such it is expressed by

$$\tau_t \propto (\tau_i + \tau_\nu + \tau_f). \tag{16}$$

Considering a certain amount of particles randomly dispersed in a liquid which produces a volumetric concentration c, Cheng [32] evaluated D_m as

$$D_m = Dc^{-\frac{1}{3}} \tag{17}$$

and therefore G_a is calculated by the following way.

$$G_a = D_m - D = D(c^{-\frac{1}{3}} - 1). \tag{18}$$

Using Eqs. (12)–(15), (17) and (18), we write Eq. (16) as

$$\tau_t = a_\tau\left[\frac{\rho_p D^2 c^{\frac{2}{3}}}{(1-c^{\frac{1}{3}})^2}\left(\frac{\partial u}{\partial y}\right)^2 + \frac{\mu_f \mu_r c^{\frac{2}{3}}}{1-c^{\frac{1}{3}}}\frac{\partial u}{\partial y} + \rho_f u_*^2(1-\xi)(1-c^{\frac{1}{3}})\right] \tag{19}$$

where a_τ is the proportionality parameter introduced here as 'velocity lag coefficient'. A suitable expression of u is required to find an explicit expression of τ_t from Eq. (19). Coles [33] proposed an analytical expression of u by including the law of wake in the widely cited expression of log-law which is not valid for the entire flow region in open channel turbulent flow. A large number of published literature has reported that the log-wake law of Coles [33] shows good agreement with a wide range of experimental data for the entire flow depth of open channel and a detailed information on this reality can be found in Dey [34]. Coleman [3] studied the effect of particles' concentration on liquid velocity through log-wake law and concluded that it can be applied for sediment-laden flow also by modified wake parameter Π varying with c; as such we consider log-wake law in our study. On the other hand, we find from published articles [35–37] that von Karman constant varies

with c and this phenomenon should be taken into account in modeling of any turbulent feature of sediment-laden flow. Therefore, the log-wake law given by Coles [33] is considered here as

$$\frac{u}{u_*} = \frac{1}{\kappa_m}\ln\xi + B_c + \frac{2\Pi}{\kappa_m}\sin^2\left(\frac{\pi}{2}\xi\right) \tag{20}$$

where κ_m is the von Karman constant of sediment–liquid mixture and B_c is a constant depending on flow conditions. The expressions of κ_m and Π varying with c are given in Appendix B. Using Eq. (20), we obtain the following normalized expression of τ_t from Eq. (19).

$$\frac{\tau_t}{\rho_f u_*^2} = a_\tau\left[\frac{(\Delta_p+1)c^{\frac{2}{3}}}{(1-c^{\frac{1}{3}})^2}\frac{D^2}{\kappa_m^2 h^2}\left(\frac{1}{\xi}+\Pi\pi\sin(\pi\xi)\right)^2 + \frac{\mu_r c^{\frac{2}{3}}}{(1-c^{\frac{1}{3}})}\frac{\nu_f}{u_*\kappa_m h}\left(\frac{1}{\xi}+\Pi\pi\sin(\pi\xi)\right) + (1-\xi)(1-c^{\frac{1}{3}})\right] \tag{21}$$

In the above paragraph, we already have obtained all the forces acting on a suspended particle and therefore we can proceed for the final expression of velocity lag. Following Cheng [22], we assume that the velocity difference between particle and liquid in sediment-laden flow is equal to the velocity lag u_l involved in Eq. (3). The drag force F_{D_m} on a suspended particle in sediment-laden flow and the surface area of that particle can be connected by

$$F_{D_m} = \tau_a\frac{\pi D^2}{4} \tag{22}$$

where the expression of τ_a needs a derivation in terms of τ_t. When a particle lies in a liquid, the upper portion of liquid on the particle plays significant role regarding the dynamics of that particle in suspension. With increasing upper portion of the flow depth, the particle experiences larger force and its motion is obstructed. This criterion can be well understood from Fig. 1. The total shear stress τ_t given by Eq. (21) describes the force per unit area acting on the particle at a given vertical height y from channel bed. To obtain the average bulk stress on that particle owing to its upper portion of flow depth, we integrate τ_t from y to h. For preserving the dimension of τ_a in Eq. (22), we divide the integration by particle diameter D for getting the average bulk stress per unit diameter and propose τ_a by

$$\tau_a = \frac{1}{D}\int_y^h \tau_t\, dy. \tag{23}$$

Using Eq. (21), we write the normalized form of τ_a from Eq. (23) as

$$\frac{\tau_a}{\rho_f u_*^2} = a_\tau\frac{h}{D}\int_\xi^1\left[\frac{(\Delta_p+1)c^{\frac{2}{3}}}{(1-c^{\frac{1}{3}})^2}\frac{D^2}{\kappa_m^2 h^2}\left(\frac{1}{\xi}+\Pi\pi\sin(\pi\xi)\right)^2 + \frac{\mu_r c^{\frac{2}{3}}}{(1-c^{\frac{1}{3}})}\frac{\nu_f}{u_*\kappa_m h}\left(\frac{1}{\xi}+\Pi\pi\sin(\pi\xi)\right) + (1-\xi)(1-c^{\frac{1}{3}})\right]d\xi \tag{24}$$

Finally, we obtain our model of velocity lag u_l from Eqs. (1)–(3), (11) and (22) as

$$\frac{u_l}{u_*} = \left[\sqrt{\left(\frac{M}{A_2}\right)^{\frac{1}{n}} + \frac{1}{4}\left(\frac{N}{A_2}\right)^{\frac{2}{n}}} - \frac{1}{2}\left(\frac{N}{A_2}\right)^{\frac{1}{n}}\right]^n \tag{25}$$

where M and N are given by

$$M = \frac{2\tau_a}{\rho_m u_*^2} \tag{26}$$

$$N = A_1\mu_r(1-c)^{\Delta_p}\frac{\nu_f}{u_* D}. \tag{27}$$

To calculate u_l from Eq. (25), the required expression of c is provided in Appendix C. At the end of the mathematical modeling of this section, we state that according to our objective, the proposed model of velocity lag is derived based on hindered drag force in sediment-laden flow, impact shear stress, viscous shear stress and turbulent shear stress which include the effects of turbulence, particle–liquid interaction, particle–particle interaction and random dispersion of suspended sediment owing to these interactions.

3. Experimental data considered for verification

After proposing the mathematical model of u_l given by Eq. (25), we have to validate it by verifying with experimental data. Due to the invention of PDA, PIV, PTV, LDA, etc. which are used to predict particle and liquid velocities separately, several experimental literature are available where u_l is measured in sediment-laden open channel turbulent flow. From the available experimental investigations, we consider data of u_l in such a way that we can show the applicability of our model for a broad range of sediment-laden flow conditions. To accomplish this task, we select experimental observation of u_l for different particles which are polystyrene [6,7], glass [9,11] and natural sand [8,12], and the flow conditions during experiments are briefly discussed as follows.

For understanding the particle–turbulence interaction, Rashidi et al. [6] conducted experiment in a 4 m long and 20 cm wide recirculating flume with varying flow parameters and we consider four experimental runs of polystyrene particle from their obtained data. In a 4.5 m long and 32 cm wide recirculating flume, Kaftori et al. [7] experimentally analyzed the behavior of polystyrene particle in turbulent boundary layer by LDA and visualization technique, and we take six experimental runs from their measured data.

Best et al. [9] predicted the turbulence modulation and the velocity of glass particle by PDA in a 10 m long and 30 cm wide recirculating flume. Righetti and Romano [11] studied the particle–fluid interaction in a 3 m long and 10 cm wide recirculating flume over a smooth bed and predicted the velocities of glass particle and liquid by PDA. Four experimental runs from Best et al. [9] and two experimental runs from Righetti and Romano [11] are selected for velocity lag data of glass particle.

Muste and Patel [8] increased concentration of sand particle successively in three experimental runs and measured particle and liquid velocities by DLDV in a 30 m long and 91 cm wide recirculating flume. We select three experimental runs of Muste and Patel [8]. Muste et al. [12] introduced a new measurement technique by combining PIV and PTV and performed experimental runs in a 6 m long and 15 cm wide recirculating flume. For velocity lag data of sand, we select three experimental runs of Muste et al. [12].

A summary of twenty-two experimental runs considered is shown in Table 1 where except the data of natural sand particle [8,12], we provide suitable names of experimental runs for polystyrene and glass particles as runs' name are not available in the corresponding literature [6,7,9,11]. We can follow from Table 1 that different flow parameters vary for a broad range in these experimental runs. To show that these runs are reasonable for verification, the explanation is given through the values of Re_A and C_{DA} in Table 1. As u_c is not available in the experimental runs, instead of calculating $\mathrm{Re}(= u_c D/\nu_f)$, we calculate averaged Reynolds number

Table 1
Summary of experimental data.

Literature	Run	D (mm)	$\Delta_p + 1$	h (cm)	U_m (cm/s)	u_* (cm/s)	ν_f (cm^2/s)	Re$_A$	C_{DA}
	Polystyrene particle								
Rashidi et al. [6]	R1	0.120	1.03	2.75	15.60	0.90	0.0084	22.3	3.42
	R2	0.220	1.03	2.75	15.60	0.90	0.0084	40.9	2.51
	R3	0.650	1.03	2.75	15.60	0.90	0.0084	120.9	1.68
	R4	1.100	1.03	2.75	15.60	0.90	0.0084	204.5	1.47
Kaftori et al. [7]	K11	0.100	1.05	3.25	24.50	1.28	0.0080	30.5	2.90
	K12	0.275	1.05	3.27	24.10	1.29	0.0079	83.5	1.89
	K13	0.900	1.05	3.27	24.85	1.34	0.0081	276.1	1.38
	K21	0.100	1.05	3.52	31.65	1.60	0.0081	39.2	2.56
	K22	0.275	1.05	3.51	32.10	1.60	0.0080	110.9	1.72
	K23	0.900	1.05	3.77	29.45	1.55	0.0078	339.8	1.33
	Glass particle								
Best et al. [9]	B1	0.125	2.60	5.75	58.00	3.40	0.0083	87.0	1.86
	B2	0.175	2.60	5.75	58.00	3.40	0.0083	121.8	1.67
	B3	0.225	2.60	5.75	58.00	3.40	0.0083	156.7	1.56
	B4	0.275	2.60	5.75	58.00	3.40	0.0083	191.5	1.49
Righetti and Romano [11]	RR1	0.100	2.60	2.30	57.00	3.29	0.0090	63.3	2.09
	RR2	0.200	2.60	2.00	60.00	3.97	0.0094	127.7	1.65
	Natural sand particle								
Muste and Patel [8]	SL01	0.230	2.65	12.90	62.90	3.02	0.0103	140.5	1.61
	SL02	0.230	2.65	12.90	62.90	3.05	0.0103	140.5	1.61
	SL03	0.230	2.65	12.80	63.30	3.13	0.0105	138.7	1.61
Muste et al. [12]	NS1	0.230	2.65	2.10	81.30	4.20	0.0093	200.4	1.47
	NS2	0.230	2.65	2.10	79.60	4.20	0.0096	191.7	1.49
	NS3	0.230	2.65	2.10	79.30	4.20	0.0091	200.2	1.47

Re$_A$($= U_m D/\nu_f$) where U_m is the mean flow velocity of sediment-laden fluid over the flow depth and the averaged drag coefficient C_{DA} is computed from Eq. (7) by replacing Re to Re$_A$. As Eq. (7) is valid for a wide range of Re($10^{-4} \leq$ Re $\leq 10^4$), Table 1 shows reasonable ranges of Re$_A$ and C_{DA} for the experimental runs. Moreover, it needs to mention that we consider the widest experimental data for the verification of the proposed model in comparison to data considered by previous researchers [20–22].

4. Assessment of our model in predicting velocity lag

We observe from most of the experimental runs of velocity lag that the measured data are very scattered; so we need to perform an assessment analysis of our velocity lag model in the determination of experimental data. For this analysis, we show the development of our model step by step and provide relevant explanation at each step. We first explain the consideration of Eq. (10) which is mentioned after this formula in Section 2. Then we give the physical justification of hindrance function H expressed by Eq. (11) and followed by a detailed discussion regarding the determination accuracy of measured velocity lag by our model.

In most of the available literatures, researchers [22,32,38] took into account the mass density ρ_m of sediment–liquid mixture by

$$\rho_m = \rho_f(1 + \Delta_p c). \tag{28}$$

We claim that Eq. (28) is confined to dilute flow only whereas Eq. (10) can be applied in both dilute and non-dilute flows. In support of our claim, we express the kinematic viscosity ν_m of sediment–fluid mixture by

$$\frac{\nu_m}{\nu_f} = \frac{\mu_m}{\rho_m}\left(\frac{\mu_f}{\rho_f}\right)^{-1} = \frac{\mu_m}{\mu_f}\left(\frac{\rho_m}{\rho_f}\right)^{-1} \tag{29}$$

where ν_f is the kinematic viscosity of particle-free liquid. Using Eqs. (10) and (28), we write the following two expressions of Eq. (29).

$$\frac{\nu_m}{\nu_f} = \frac{\mu_m}{\mu_f(1 + \Delta_p c)} \tag{30}$$

$$\frac{\nu_m}{\nu_f} = \frac{\mu_m}{\mu_f(1 - c)^{-\Delta_p}}. \tag{31}$$

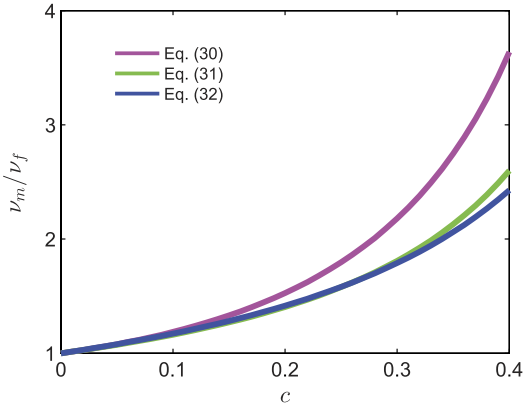

Fig. 2. Variation of ν_m with c for Eqs. (30)–(32).

Expression on ν_m is rarely found in the literature and therefore we select the available following formula of ν_m by Sha [39].

$$\frac{\nu_m}{\nu_f} = \left(1 - \frac{c}{c_m}\right)^{-1} \tag{32}$$

where the maximum volumetric concentration c_m is taken as 2/3 following Cheng [38] who evaluated it by packing uniform spheres in a cylinder with unit length and the same diameter of sphere. Considering Eq. (32) as reference, we show the comparison of Eqs. (30) and (31) in Fig. 2. We notice that though Eq. (30) deviates from Eq. (32) after $c = 0.15$, Eq. (31) shows reasonable agreement with Eq. (32) for $0 \leq c \leq 0.5$ which leads to the inference that ρ_m expressed by Eq. (10) is well applicable for both dilute and non-dilute flows rather than Eq. (28) for dilute flow only.

In this paragraph, we describe the physical justification of our hindrance function H expressed by Eq. (11). The proposed expression of H is a function of mass density ρ_p of particle in terms of Δ_p, particle Reynolds number Re and particles' concentration c. The variation of H with c for different values of Re and Δ_p is depicted in Fig. 3. We follow that for fixed values of c and Re, H increases with increasing Δ_p and therefore the increased hindered drag force

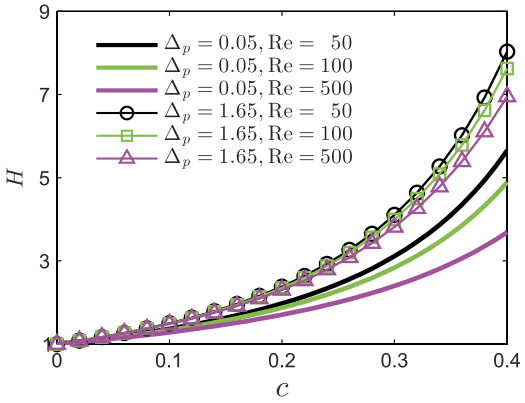

Fig. 3. Variation of H with c for different values of Δ_p and Re.

F_{D_m} in sediment-laden flow is obtained through Eq. (2). The natural reason is that ρ_p increases in terms of Δ_p and consequently higher drag force is required to drag the particle with the liquid flow in the suspension region. Another natural characteristic of velocity lag u_l for a particle with fixed concentration is that it increases with decreasing value of F_{D_m} as decreased hindered drag force is not able to accelerate the particle with the liquid flow. We also can explain this phenomenon from Eq. (11) as follows. For fixed value of c, increasing value of u_l implies increased u_c by Eq. (5) and it leads to an increasing value of Re through Eq. (6). Fig. 3 displays that with increasing Re, H decreases and results decreased F_{D_m} which is the expected outcome. It is also depicted in Fig. 3 that the value of H increases with increasing c irrespective of Re and Δ_p. The reason behind this fact is that with increasing c, the flow path of a particle in a certain domain is obstructed by more number of other suspended particles and therefore increased F_{D_m} is required through increased value of H to accelerate the particle with liquid velocity in that flow region. It is worthwhile to mention that Eq. (11) is not valid at $c = 1$ which represents a solid state without liquid and the investigation of velocity lag is not required. From the above discussion, we claim that the proposed hindrance function H is physically correct due to explaining real phenomena of particle's dynamics in flow region.

After giving the physical justification of H, it remains to provide an explanation on the prediction ability of our model to estimate the measured velocity lag data. It is required to mention here that most of the observed data of velocity lag are very scattered; hence its prediction by a mathematical equation becomes very difficult as any dependent variable in an equation does not follow zigzag pattern with the variation of its independent variables. In spite of the scattered pattern of data, we choose comparatively three consistent experimental runs R1, RR2, NS1 of velocity lag for polystyrene, glass and sand particles respectively to show the determination ability of the present model. We derive our model based on four hydrodynamic mechanisms which are hindered drag force, impact shear stress, viscous shear stress and turbulent shear stress and these features are structured through the effects of turbulence, particle–liquid interaction, particle–particle interaction and random dispersion of suspended sediment owing to these interactions. For calculating velocity lag from the proposed model given by Eq. (25), the parameter a_τ is required to be estimated only from experimental data. We show the computed velocity lag profiles from Eq. (25) and measured data simultaneously in Fig. 4. It is observed that our model follows the pattern of experimental data and it can be predicted quite well by adjusting the value of a_τ. The reason behind the efficiency of our model in estimating experimental data can be explained as follows. The present model of u_l is derived through a proper formulation of H together with an appropriate expression of ρ_m valid for both dilute and non-dilute sediment-laden flows. In addition, all the influential shear stresses τ_i, τ_v and τ_f are considered together with several crucial interaction dynamics of liquid and particle in suspension region. In contrast to this fact, previous researchers considered only limited underlying physics of flow region in their models of velocity lag; accordingly these models either underestimate or overestimate the measured data in most of the cases and this fact can be well understood from the next section by comparison analysis between experimental data, present model and other existing models considered for comparison with the present model. Towards the end of this section, we can assert that our model has good potential in estimating experimental observations of velocity lag in spite of scattered and zigzag natures of data.

5. Comparison with experimental data and other existing models

In this section, we verify our model of velocity lag u_l with the experimental data considered and also compare our model with other existing models. For calculating u_l from Eq. (25), the value of the unknown parameter velocity lag coefficient a_τ is required and we estimate it for each experimental run when adequate agreement is observed between computed and observed values of normalized velocity lag u_l/u_*. We notice that the fitted values of a_τ depends on fluid flux, particle diameter D and mass density ρ_p of particle in terms of Δ_p. We carry out a regression analysis on the fitted values of a_τ and obtain the following formula.

$$a_\tau = 618.741\ (\Delta_p + 1)^{2.450} \left(\frac{u_*}{\omega_p}\right)^{0.812} \left(\frac{D}{h}\right)^{1.896}. \tag{33}$$

We observe from Fig. 5 that the computed values of a_τ from Eq. (33) provide good agreement with the fitted values of a_τ together with $R^2 = 0.9007$. The suggested formula of a_τ given by Eq. (33) confirms no estimation of empirical parameter to calculate velocity lag from our model. Apart from the agreement analysis between experimental data and our model, we compare it with other existing velocity lag models. We would like to mention that explicit expressions on velocity lag available in the literature are few and we

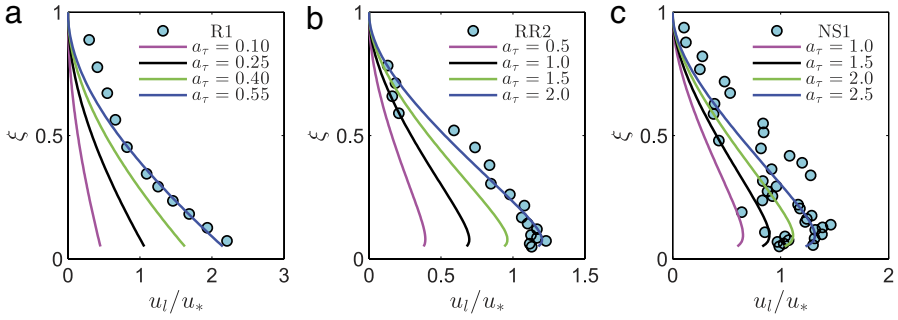

Fig. 4. Assessment of present velocity lag model given by Eq. (25) in predicting experimental data.

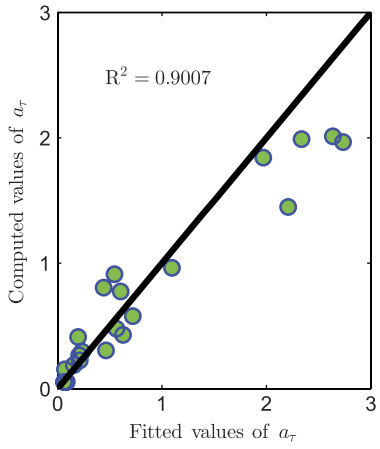

Fig. 5. Comparison between computed values of a_τ from Eq. (33) and fitted values of a_τ.

choose the existing models of Cheng [22] and Greimann et al. [20]. The expression of Cheng [22] model is

$$\frac{u_l}{u_*} = \left[\sqrt{(2-2\xi)^{\frac{1}{1.5}} + \frac{1}{4}\left(32\frac{\nu_f}{u_* D}\right)^{\frac{2}{1.5}}} - \frac{1}{2}\left(32\frac{\nu_f}{u_* D}\right)^{\frac{1}{1.5}}\right]^{1.5} \quad (34)$$

and the formula of Greimann et al. [20] model is

$$\frac{u_l}{u_*} = 0.66\frac{\omega_p}{u_*}(1-\xi)\exp(1.34\xi). \quad (35)$$

For the following discussion on comparison analysis, the models of present study, Cheng [22] and Greimann et al. [20] are denoted by PM, CM and GM respectively.

For polystyrene particle, the comparisons of u_l between experimental data and computed values from PM, CM and GM are shown in Figs. 6–8 in which Fig. 6 stands for Rashidi et al. [6] data and Figs. 7 and 8 represent the comparison of Kaftori et al. [7] data for $U_m \approx 24$ and 31 cm/s respectively. We observe from Figs. 6–8 that PM shows good agreement with experimental data whereas CH and GM highly underestimate the data.

For glass particle, we depict the comparison between observed and computed values of u_l in Figs. 9 and 10 for Best et al. [9] and Righetti and Romano [11] data respectively. Fig. 9 shows that all theoretical models provide reasonable agreement with Best et al. [9] data. On the other hand PM matches well with Righetti and Romano [11] data in Fig. 10 whereas CM and GM underestimate that measured data.

For natural sand particle, Figs. 11 and 12 exhibit the comparison between computed and measured values of u_l for Muste and Patel [8] data and Muste et al. [12] data respectively. We notice from Fig. 11 that though PM and CM predict the data of Muste and Patel [8] well, GM overestimates that data. We also follow from Fig. 12 that PM agrees well with Muste et al. [12] data whereas CM and GM give underestimated values.

Apart from these graphical representations, we carry out a detailed error analysis to examine the estimation accuracy of our model with respect to other models considered for comparison. As the experimental data of velocity lag are highly scattered, we need a suitable error formula. In this context, we select the root-mean-square error E given by

$$E = \sqrt{\frac{1}{N}\sum_{i=1}^{N}(V_{ci} - V_{oi})^2} \quad (36)$$

where V_{ci} and V_{oi} are computed and observed values of the ith data point of normalized velocity lag (u_l/u_*) in a run and N is the total number of data points in that run. For each experimental run, the computed values of E from GM, CH and PM are displayed in Table 2 where star $(*)$ denotes the least error for that run. We observe from Table 2 that our model provides least error for twenty cases out of twenty-two experimental runs considered. This fact assures the superior determination accuracy of our model in comparison to existing models of Greimann et al. [20] and Cheng [22].

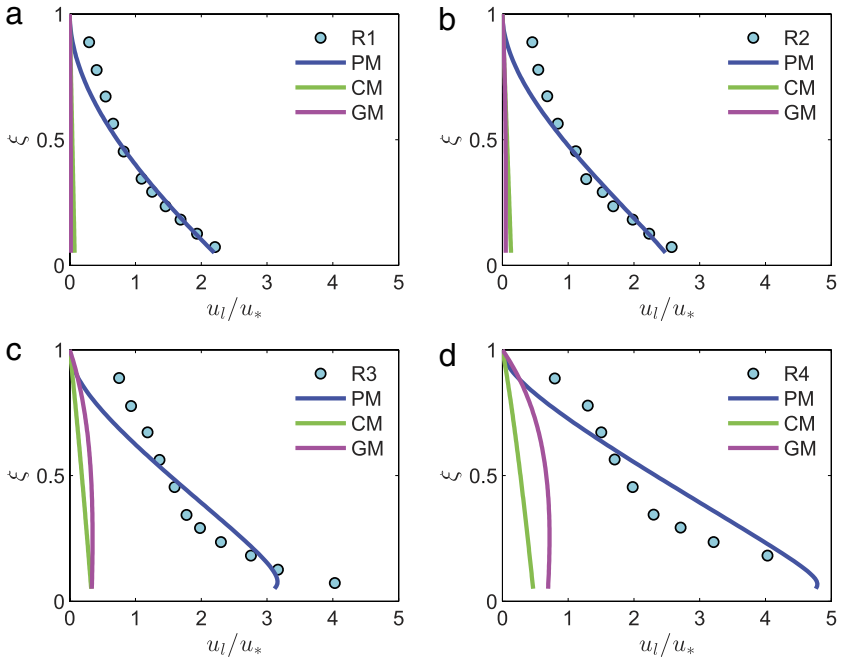

Fig. 6. For experimental runs (a) R1, (b) R2, (c) R3 and (d) R4 of Rashidi et al. [6], comparison of velocity lag u_l between observed and computed values from PM, CM and GM given by Eqs. (25), (34) and (35) respectively.

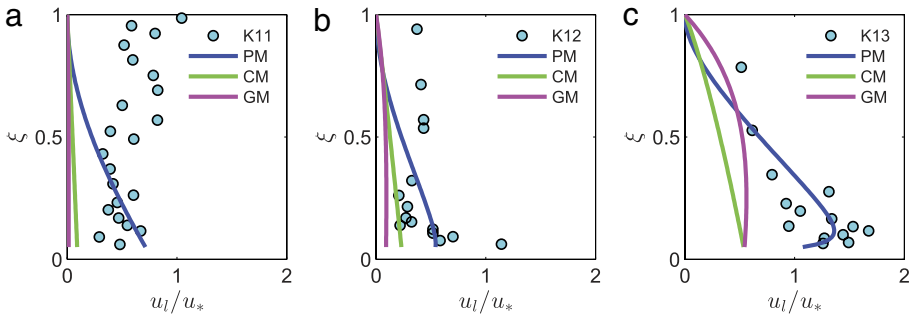

Fig. 7. For experimental runs (a) K11, (b) K12 and (c) K13 of Kaftori et al. [7], comparison of velocity lag u_l between observed and computed values from PM, CM and GM given by Eqs. (25), (34) and (35) respectively.

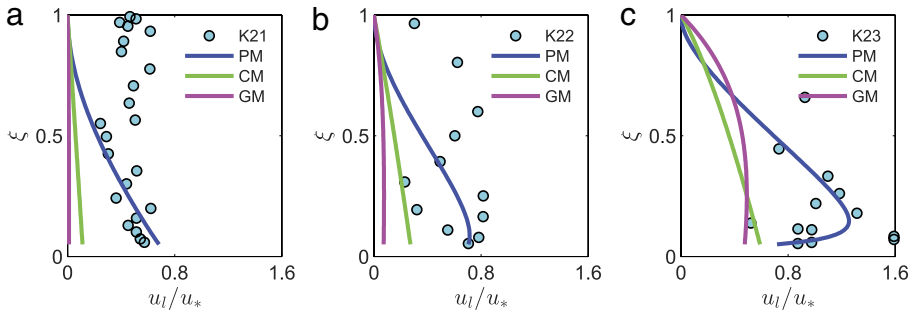

Fig. 8. For experimental runs (a) K21, (b) K22 and (c) K23 of Kaftori et al. [7], comparison of velocity lag u_l between observed and computed values from PM, CM and GM given by Eqs. (25), (34) and (35) respectively.

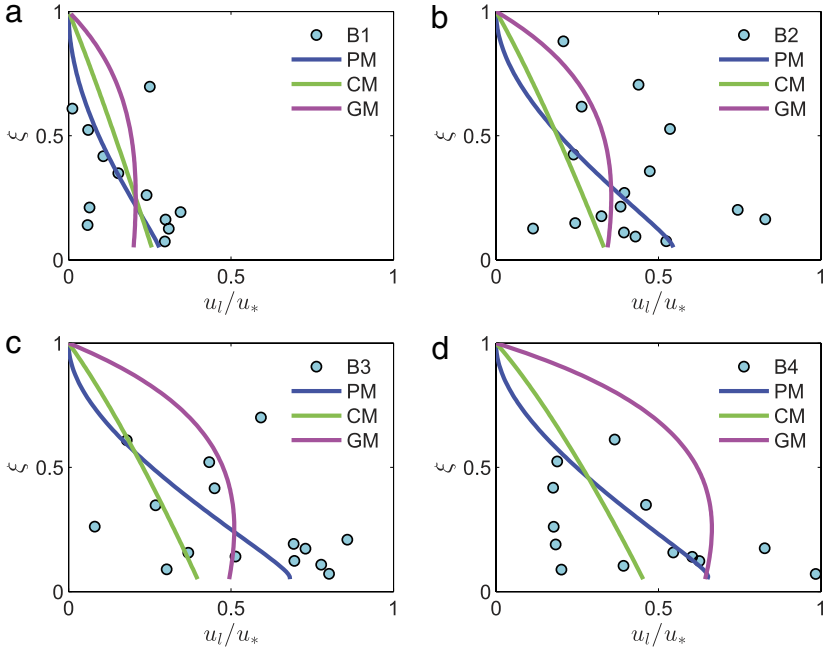

Fig. 9. For experimental runs (a) B1, (b) B2, (c) B3 and (d) B4 of Best et al. [9], comparison of velocity lag u_l between observed and computed values from PM, CM and GM given by Eqs. (25), (34) and (35) respectively.

6. Discussions

After the comparison analysis done minutely in the previous section, we need to discuss the physical justification of the model as well as its performance. The physical justification is provided in Section 6.1 through explaining the real phenomena of velocity lag owing to particle–liquid interaction by our model. We demonstrate the better performance of our model in Section 6.2 from several aspects by comparing it with existing models.

6.1. Rationalization of explaining real phenomena of velocity lag

Here we give a detailed interpretation on the rational explanation of real phenomena of velocity lag by our model from Eq. (25) together with Eq. (33). During comparison analysis in Section 5, we notice that D, ρ_p and u_* play significant role in our model. The ability of describing real phenomena of velocity lag by our model is done by studying the effects of these parameters on the model. To do this analysis, we arbitrarily choose an experimental run for

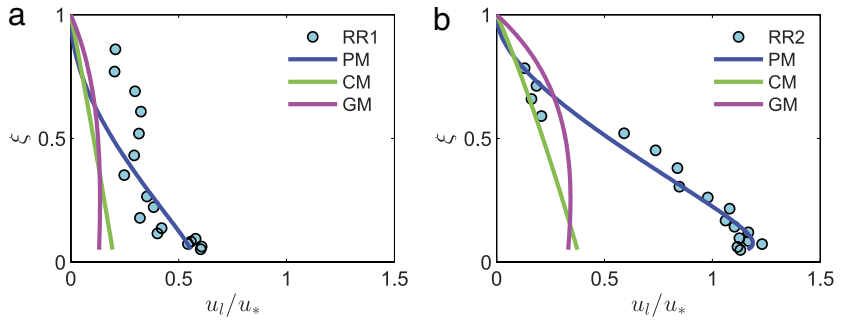

Fig. 10. For experimental runs (a) RR1 and (b) RR2 of Righetti and Romano [11], comparison of velocity lag u_l between observed and computed values from PM, CM and GM given by Eqs. (25), (34) and (35) respectively.

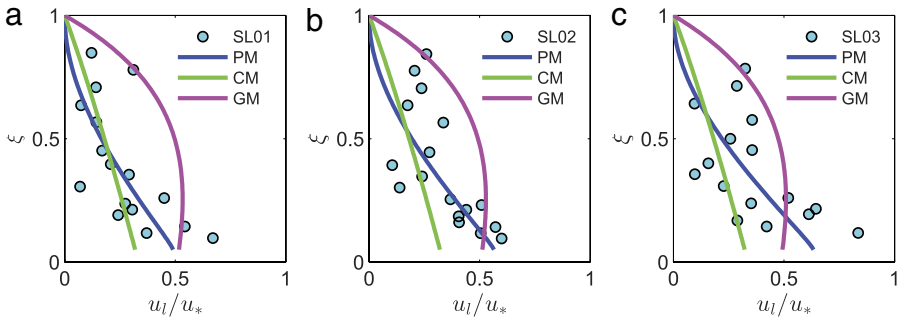

Fig. 11. For experimental runs (a) SL01, (b) SL02 and (c) SL03 of Muste and Patel [8], comparison of velocity lag u_l between observed and computed values from PM, CM and GM given by Eqs. (25), (34) and (35) respectively.

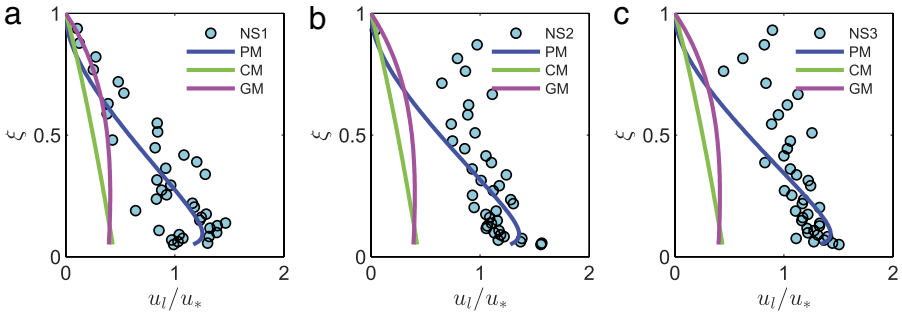

Fig. 12. For experimental runs (a) NS1, (b) NS2 and (c) NS3 of Muste et al. [12], comparison of velocity lag u_l between observed and computed values from PM, CM and GM given by Eqs. (25), (34) and (35) respectively.

the values of other parameters associated in the model and then vary each of the three aforementioned parameters by keeping others constant.

We depict the effect of particle diameter D on velocity lag u_l in Fig. 13 and follow that it increases with increasing D. The values of mass and surface area of a particle increase with increasing D, thus it accelerates less with the liquid velocity and results increased u_l. This characteristic is also matched with the experimental result of Rashidi et al. [6] who obtained increasing u_l with increasing D by keeping other parameters fixed and this fact is well understood from Table 1 and Fig. 6.

We illustrate the effect of mass density ρ_p of particle in terms of Δ_p in Fig. 14 and notice that u_l increases with increasing Δ_p. The mass of sediment particle increases with increasing Δ_p which results the requirement of more force to accelerate it with the liquid flow. As the stress is same due to same liquid flux, heavy particle accelerates less than the liquid velocity in comparison to finer particle and a higher value of velocity lag u_l is obtained. This result also agrees with the experimental investigation of Muste et al. [12] who performed experiments with crushed nylon (Δ_p = 0.03) and natural sand (Δ_p = 1.65) and obtained larger value of u_l for sand particle.

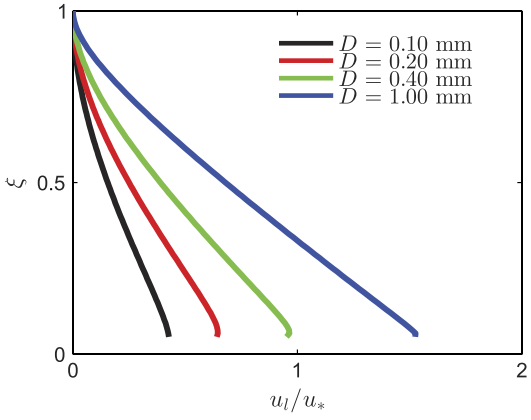

Fig. 13. Effect of D on u_l profile computed from Eq. (25) together with Eq. (33).

Table 2
Calculated values of E from different models.

Literature	Run	GM	CH	PM
Rashidi et al. [6]	R1	1.27	1.23	0.14*
	R2	1.47	1.43	0.19*
	R3	1.91	1.98	0.44*
	R4	2.76	3.05	0.88*
Kaftori et al. [7]	K11	0.59	0.56	0.46*
	K12	0.43	0.35	0.26*
	K13	0.66	0.76	0.22*
	K21	0.47	0.42	0.32*
	K22	0.56	0.44	0.30*
	K23	0.61	0.61	0.36*
Best et al. [9]	B1	0.11	0.10*	0.10*
	B2	0.19*	0.24	0.22
	B3	0.23*	0.30	0.24
	B4	0.37	0.30*	0.30*
Righetti and Romano [11]	RR1	0.29	0.26	0.11*
	RR2	0.59	0.60	0.08*
Multe and Patel [8]	SL01	0.27	0.14	0.13*
	SL02	0.21	0.17	0.12*
	SL03	0.23	0.22	0.17*
Muste et al. [12]	NS1	0.60	0.66	0.21*
	NS2	0.70	0.77	0.32*
	NS3	0.75	0.81	0.33*

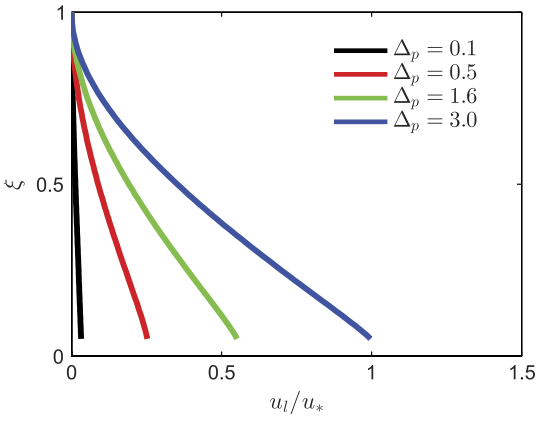

Fig. 14. Effect of Δ_p on u_l profile computed from Eq. (25) together with Eq. (33).

We demonstrate the effect of fluid flux in terms of shear velocity u_* on u_l profile in Fig. 15 where each profile is normalized by the corresponding value of u_*. It is observed that u_l decreases with increasing u_*. The simple reason is that the increased shear stress with increasing liquid velocity in terms of u_* leads the particle to follow the velocity of liquid and decreased u_l is obtained. Though a logical effect of u_* is found, still we cannot verify this phenomenon with measured data as the variation of u_* is negligible in the experimental runs considered in this study for verification.

We end up this section by saying that our model of velocity lag rationalizes the real phenomenological characteristics of velocity lag caused by the interaction between particle and liquid during turbulent flow and this ability justifies the physical correctness of our model.

6.2. Advantage of our model

This section demonstrates the excellency of our model from several aspects in comparison to other existing models. At first, it needs to mention that irrespective of the amount of particles in sediment-laden open channel turbulent flow, the concentration is always high near the channel bed; as a result impact shear stress τ_i and viscous shear stress τ_v inherently occur there due to particle–particle and particle–liquid interactions respectively.

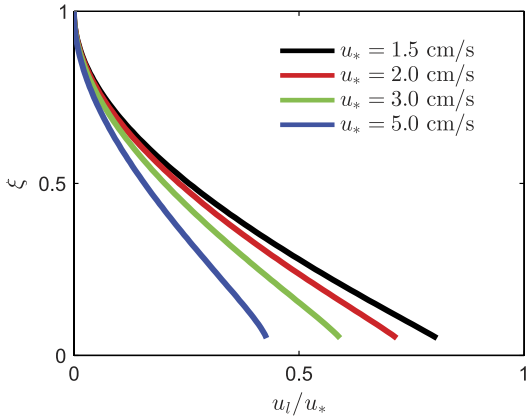

Fig. 15. Effect of u_* on u_l profile computed from Eq. (25) together with Eq. (33).

Apart from this, turbulent shear stress τ_f plays a crucial role in the entire suspension region of turbulent flow and the drag force on suspended particle has enormous importance to accelerate that particle with liquid velocity. Moreover, the magnitudes of these forces along vertical direction in the suspension region alter at high concentration. By keeping in mind these mentioned physics of flow region, we formulate our model of velocity lag u_l based on hindered drag force in sediment-laden flow, τ_i, τ_v and τ_f together with the inclusion of effects of turbulence, particle–liquid interaction, particle–particle interaction and random dispersion of suspended sediment owing to these interactions. The mathematical formulae in this study to express those turbulent features are valid for both dilute and non-dilute sediment-laden flows. Due to considering several turbulent features, our model assesses the experimental data in a quite reasonable way at Section 4 in spite of the scattered and zigzag nature of data. On the other hand, the models of Greimann et al. [20] and Cheng [22] show concave and linear shapes respectively and it can be observed in Figs. 6–12. Therefore, these models either underestimate or overestimate experimental data and the reason might be inclusion of limited consideration of underlying physics in sediment-laden flow region and the applicability of these models is to be suspected when significant gradients of liquid velocity and particles' concentration exist in the flow. Next, we want to elucidate that due to the random fluctuation characteristic of sediment-laden flow, it is very challenging to derive a theoretical model of any turbulent feature without any empirical parameter and the application of a theoretical model is not an easy task when several empirical parameters are needed to be estimated from experimental data. This fact can be followed from the u_l profile suggested by Jiang et al. [21]. In contrast, the major advantage in our model is that no empirical parameter is required to be estimated from experimental data for a wide range of flow conditions. In addition, the error analysis shown in Table 2 secures the superior determination accuracy of our model in comparison to other existing models to approximate experimental data. Due to the inclusion of several physics of sediment-laden flow in our model and its superior ability in computing experimental data, we remark at the end of this paragraph that our model can be applied to compute u_l for a wide applicable region for both dilute and non-dilute sediment-laden flows.

Apart from the above discussion on assessment analysis and applicable region, we mention that the profile of u_l given by Cheng [22] shows inconsistent behavior with varying particle diameter and showed negligible variation with changing mass density of particle. To observe these outcomes, we refer the corresponding graphical representations in Cheng [22]. These outcomes are not logical according to experimental observations [6,12] and the results obtained in Section 6.1 where our model shows consistent behavior by varying those parameters and rationalizes real

phenomena of velocity lag owing to particle–liquid interaction in flow region. On the other hand, we acquaint with an interesting characteristic of our model for some experimental runs e.g. K11 and NS2 in Figs. 7 and 12 respectively that it cannot estimate the measured data far from the channel bed due to decreasing calculated values of u_l from Eq. (25) with increasing normalized vertical height ξ from channel bed. We envisage that it is not a limitation of this present model. The decreasing characteristic of u_l with increasing ξ is logical and it can be explained as follows. It is a well known fact that the volumetric concentration c of particle decreases with increasing ξ and it results $u_l > u_c$ from Eq. (5) as $0 < c < 1$. As c tends to 0 with increasing ξ, the velocity lag u_l in sediment-laden flow converges to the velocity lag u_c between liquid and particle in particle-free flow and therefore decreased u_l in particle-laden flow is obtained. We also would like to say that the deviation of our model from experimental data at the upper portion of flow depth are not found globally for all experimental runs of velocity lag; as such this phenomenon can be treated as experimental error commonly found in the experiments related to open channel turbulent flow. The present model has a noticeable ability to explain real phenomena of velocity lag in a comprehensive logical way.

At the end, we have to address the significance of our model in terms of its utilization in the branch of fluvial hydraulics. The present model would help in calculating velocity lag for a wide range of flow conditions through rigorous numerical solution procedures from two-phase flow approach. Also, the streamwise velocity profile u_p of particle in suspension region can be obtained easily if the streamwise velocity profile u of liquid in sediment-laden flow is known to us.

7. Conclusions

From theoretical point of view, a mathematical model of velocity lag between particle and liquid in sediment-laden open channel turbulent flow is proposed. The model is derived on the basis of hindered drag force in sediment-laden fluid, impact shear stress, viscous shear stress and turbulent shear stress which include the effects of turbulence, particle–particle interaction, particle–liquid interaction and random dispersion of suspended particles caused by these interactions. As these interactions are very prominent at high concentration, the model can be applicable for both dilute and non-dilute sediment-laden flows. No empirical parameter needs to be estimated for calculating velocity lag and it is a major advantage of the model. Unlike the previous researchers, a broad range of experimental data collected from published literature is considered for the verification of the model. In spite of the scattered and zigzag patterns of measured data, these experimental observations are assessed quite well by the present model. A detailed error analysis confirms the superior prediction accuracy of our model in comparison to other existing models of velocity lag. The present model rationalizes the real phenomena of velocity lag owing to the particle–liquid interaction in turbulent flow. Due to the aforementioned abilities, we conclude towards the end of this study that the present model can be used to predict velocity lag for a broad flow field in sediment-laden open channel turbulent flow.

Acknowledgment

We express our sincere thanks to reviewers for their constructive suggestions to improve the manuscript.

Appendix A. Dynamic viscosity μ_m of sediment–fluid mixture

An appropriate expression of dynamic viscosity $\mu_m (= \mu_f \mu_r)$ of sediment–liquid mixture is needed to calculate the u_l from Eq. (25). Several expressions of μ_m in terms of particles' concentration c are available in literature [40–42]. Among these formulae, we select the equation of μ_m by Leighton and Acrivos [41] as it is evaluated on the basis of shear induced migration of particle in concentrated suspension and suitable also for this study. The expression of μ_m is suggested by

$$\mu_r = \frac{\mu_m}{\mu_f} = \left[1 + \frac{0.5[\mu]c}{1 - \frac{c}{c_m}}\right]^2 \tag{A.1}$$

where the intrinsic viscosity $[\mu]$ denotes the contribution of sediment to increase the viscosity of sediment–liquid mixture. It is treated as an empirical parameter and we take its value as 3 suggested in Leighton and Acrivos [41].

Appendix B. Formulae of κ_m and Π in sediment–liquid mixture

It is a well known fact that with varying c, von Karman constant κ_m and wake parameter Π change in sediment-laden flow [35–37,34] though mathematical expressions on these parameters in existing literature are very few. If we consider those existing formulae in Eq. (20), then $\partial c/\partial y$ occurs in Eq. (21) through $\partial u/\partial y$ in Eq. (19) and a rigorous numerical solution procedure is required to preform the integration given by Eq. (24) and this fact results to face a huge difficulty in computing u_l from Eq. (25). To overcome this difficulty, we replace c by particles' averaged concentration $\bar{c}$ given by $\bar{c} = (1 - \xi_a)^{-1} \int_{\xi_a}^{1} c \, d\xi$ where the normalized reference level ξ_a is discussed in the next section. Among the existing expression of κ_m, we select the formula of Yang [35] as it has reasonable prediction accuracy for a wide range of experimental data. By replacing c to $\bar{c}$, the formula of κ_m given by Yang [35] is suggested as

$$\kappa_m = \kappa \left(1 - \frac{0.14\bar{c}^{1/3}}{c_m^{1/3} - \bar{c}^{1/3}}\right) \tag{B.1}$$

where the universal value of von Karman constant κ for particle-free liquid is taken as 0.4. On the other hand, most of the existing formulae [35,43] on Π are suggested in terms of Richardson number; hence the utilization of these formula in our study is a hard task. As a solution, we collect the values of $\bar{c}$ and Π from Parker and Coleman [44] and derive the following regression equation for a wide range of particles' concentration.

$$\Pi = 1.13\bar{c} + 0.34. \tag{B.2}$$

Reasonable agreement is followed in Fig. B.16 between estimated value of Π and Eq. (B.2).

Appendix C. Profile of volumetric concentration c

A suitable expression of c is required to perform the integration for calculating τ_a as well as velocity lag u_l expressed by Eqs. (24) and (25) respectively. We include the effects of particle–particle and particle–liquid interactions in our model of u_l and want to apply it for both dilute and non-dilute sediment-laden flows, thus we select the formula of c by Hunt [45]. The expression of c is suggested by

$$\frac{c}{1-c} = \left(\frac{c_a}{1-c_a}\right)\left(\frac{\xi_a}{1-\xi_a}\frac{1-\xi}{\xi}\right)^{\frac{\omega_p}{\kappa u_*}} \tag{C.1}$$

where ω_p is the settling velocity of sediment particle in clear still liquid, $\xi_a (= a/h)$ is the normalized reference level in which a is the dimensional reference level or bed load layer thickness and c_a is the reference concentration or equilibrium near-bed concentration at ξ_a.

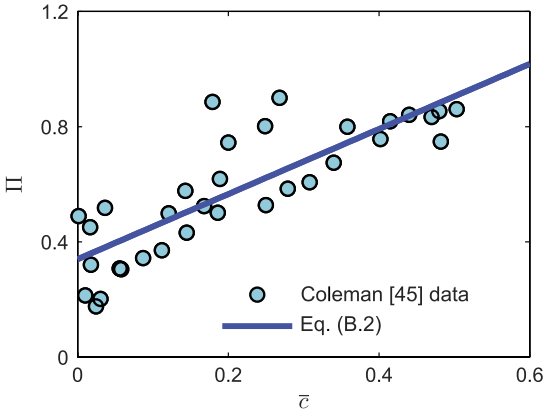

Fig. B.16. Comparison between estimated Π of Parker and Coleman [44] and Eq. (25).

To determine c, we need explicit expressions of ω_p, a and c_a as the values of these parameters are not available in most of the experimental runs considered for verification. The settling velocity ω_p of particle plays significant role in the downward gravitational settlement of sediment and for the expression of ω_p, we choose the following widely cited formula of Cheng [24].

$$\omega_p = \frac{\nu_f}{D}\left(\sqrt{25 + 1.2D_*^2} - 5\right)^{1.5}. \tag{C.2}$$

The well known expression of normalized particle diameter D_* in Eq. (C.2) is

$$D_* = \left(\frac{\Delta_p g}{\nu_f^2}\right)^{\frac{1}{3}} D \tag{C.3}$$

where g is the gravitational acceleration. The reference level a which locates the equilibrium position between bed load and suspended load equals to few diameters of sediment particle. We take the value of a as 5% of flow depth h and it is quite reasonable value. The reference concentration c_a at a represents the equilibrium near-bed concentration between bed load and suspended load. Balancing the entrainment and deposition of sediment near the bed, Cao [46] suggested c_a by

$$c_a = \frac{c_b}{160}\frac{D}{h}\frac{U_m}{\omega_p}\left(\frac{\tau_*}{\tau_{*c}} - 1\right)\left(\frac{D}{\nu_f}\sqrt{\Delta_p g D}\right)^{0.8} \tag{C.4}$$

where c_b is the bed concentration and its value is considered as 0.6 following Cao [46], U_m is the mean flow velocity over the flow depth, $\tau_*(= u_*^2/[\Delta_p g D])$ is the normalized shear stress and τ_{*c} is the normalized critical shear stress for the incipient motion of sediment particle. Soulsby and Whitehouse [47] accumulated some fundamental issues related to the initial movement of sediment particle and proposed τ_{*c} by

$$\tau_{*c} = \frac{0.24}{D_*} + 0.055[1 - \exp(-0.02D_*)] \tag{C.5}$$

References

[1] V.A. Vanoni, Transportation of suspended sediment by water, Trans. Am. Soc. Civ. Eng. 111 (1) (1946) 67–102.
[2] H.A. Einstein, N. Chien, Effects of Heavy Sediment Concentration Near the Bed on Velocity and Sediment Distribution, Missoury River Div., U. S. Corps of Engineers, 1955.
[3] N.L. Coleman, Effects of suspended sediment on the open-channel velocity distribution, Water Resour. Res. 22 (10) (1986) 1377–1384.
[4] W. Xingkui, Q. Ning, Turbulence characteristics of sediment-laden flow, J. Hydraul. Eng. 115 (6) (1989) 781–800.
[5] M. Bouvard, S. Petkovic, Vertical dispersion of spherical, heavy particles in turbulent open channel flow, J. Hydraul. Res. 23 (1) (1985) 5–20.
[6] M. Rashidi, G. Hetsroni, S. Banerjee, Particle-turbulence interaction in a boundary layer, Int. J. Multiph. Flow 16 (6) (1990) 935–949.
[7] D. Kaftori, G. Hetsroni, S. Banerjee, Particle behavior in the turbulent boundary layer. ii. velocity and distribution profiles, Phys. Fluids 7 (5) (1995) 1107–1121.
[8] M. Muste, V.C. Patel, Velocity profiles for particles and liquid in open-channel flow with suspended sediment, J. Hydraul. Eng. 123 (9) (1997) 742–751.
[9] J. Best, S. Bennett, J. Bridge, M. Leeder, Turbulence modulation and particle velocities over flat sand beds at low transport rates, J. Hydraul. Eng. 123 (12) (1997) 1118–1129.
[10] K.T. Kiger, C. Pan, Suspension and turbulence modification effects of solid particulates on a horizontal turbulent channel flow, J. Turbul. 3 (19) (2002) 1–17.
[11] M. Righetti, G.P. Romano, Particle–fluid interactions in a plane near-wall turbulent flow, J. Fluid Mech. 505 (2004) 93–121.
[12] M. Muste, K. Yu, I. Fujita, R. Ettema, Two-phase versus mixed-flow perspective on suspended sediment transport in turbulent channel flows, Water Resour. Res. 41 (10) (2005) W10402.
[13] K. Noguchi, I. Nezu, Particle–turbulence interaction and local particle concentration in sediment-laden open-channel flows, J. Hydro-Environ. Res. 3 (2) (2009) 54–68.
[14] N.B. Tuyen, N.S. Cheng, A single-camera technique for simultaneous measurement of large solid particles transported in rapid shallow channel flows, Exp. Fluids 53 (5) (2012) 1269–1287.
[15] J. Chauchat, S. Guillou, On turbulence closures for two-phase sediment-laden flow models, J. Geophys. Res. Oceans, 113 (C11017).
[16] F.A. Bombardelli, S.K. Jha, Hierarchical modeling of the dilute transport of suspended sediment in open channels, Environ. Fluid Mech. 9 (2) (2009) 207–235.
[17] S.K. Jha, F. Bombardelli, Two-phase modeling of turbulence in dilute sediment-laden, open-channel flows, Environ. Fluid Mech. 9 (2) (2009) 237–266.
[18] S. Elghobashi, On predicting particle-laden turbulent flows, Appl. Sci. Res. 52 (4) (1994) 309–329.
[19] S.K. Jha, F. Bombardelli, Toward two-phase flow modeling of nondilute sediment transport in open channels, J. Geophys. Res. Earth Surf. 115 (F03015).
[20] B.P. Greimann, M. Muste, F.M. Holly Jr., Two-phase formulation of suspended sediment transport, J. Hydraul. Res. 37 (4) (1999) 479–500.
[21] J. Jiang, A.W.K. Law, N.S. Cheng, Two-phase modeling of suspended sediment distribution in open channel flows, J. Hydraul. Res. 42 (3) (2004) 273–281.
[22] N.S. Cheng, Analysis of velocity lag in sediment-laden open channel flows, J. Hydraul. Eng. 130 (7) (2004) 657–666.
[23] R.Di Felice, The voidage function for fluid-particle interaction systems, Int. J. Multiph. Flow 20 (1) (1994) 153–159.
[24] N.S. Cheng, Simplified settling velocity formula for sediment particle, J. Hydraul. Eng. 123 (2) (1997) 149–152.
[25] D. Pal, K. Ghoshal, Hindered settling with an apparent particle diameter concept, Adv. Water Resour. 60 (2013) 178–187.
[26] R.A. Bagnold, Experiments on a gravity-free dispersion of large solid spheres in a newtonian fluid under shear, Proc. R. Soc. Lond. Ser. A Math. Phys. Eng. Sci. 225 (1160) (1954) 49–63.
[27] K. Ghoshal, D. Pal, An analytical model for bedload layer thickness, Acta Mech. 225 (3) (2013) 701–714.
[28] W.C. Mih, An empirical shear stress equation for general solid-fluid mixture flows, Int. J. Multiph. Flow 19 (4) (1993) 683–690.
[29] M. Cellino, W. Graf, Sediment-laden flow in open-channels under noncapacity and capacity conditions, J. Hydraul. Eng. 125 (5) (1999) 455–462.
[30] S. Kundu, K. Ghoshal, Effects of secondary current and stratification on suspension concentration in an open channel flow, Environ. Fluid Mech. 14 (6) (2014) 1357–1380.
[31] W.C. Mih, High concentration granular shear flow, J. Hydraul. Res. 37 (2) (1999) 229–248.
[32] N.S. Cheng, A diffusive model for evaluating thickness of bedload layer, Adv. Water Resour. 26 (8) (2003) 875–882.
[33] D. Coles, The law of the wake in the turbulent boundary layer, J. Fluid Mech. 1 (2) (1956) 191–226.
[34] S. Dey, Fluvial Hydrodynamics: Hydrodynamic and Sediment Transport Phenomena, Springer, 2014.
[35] S.Q. Yang, Turbulent transfer mechanism in sediment-laden flow, J. Geophys. Res. Earth Surf. 112 (F1).
[36] R. Gaudio, A. Miglio, S. Dey, Non-universality of von kármán's κ in fluvial streams, J. Hydraul. Res. 48 (5) (2010) 658–663.
[37] O. Castro-Orgaz, J.V. Giráldez, L. Mateos, S. Dey, Is the von kármán constant affected by sediment suspension?, J. Geophys. Res. Earth Surf. 117 (F4).
[38] N.S. Cheng, Effect of concentration on settling velocity of sediment particles, J. Hydraul. Eng. 123 (8) (1997) 728–731.
[39] Y. Sha, Basic principles of sediment transport, J. Sedim. Res. 1 (2) (1956) 1–54. in Chinese.
[40] A.B. Metzner, Rheology of suspensions in polymeric liquids, J. Rheol. 29 (6) (1985) 739–775.
[41] D. Leighton, A. Acrivos, The shear-induced migration of particles in concentrated suspensions, J. Fluid Mech. 181 (1) (1987) 415–439.

[42] C.U. Thomas, M. Muthukumar, Convergence of multiple scattering series for two-body hydrodynamic effects on shear viscosity of suspensions of spheres, J. Chem. Phys. 94 (6) (1991) 4557–4567.
[43] S. Kundu, K. Ghoshal, An explicit model for concentration distribution using biquadratic-log-wake law in an open channel flow, J. Appl. Fluid Mech. 6 (3) (2013) 339–350.
[44] G. Parker, N.L. Coleman, Simple model of sediment-laden flows, J. Hydraul. Eng. 112 (5) (1986) 356–375.
[45] J.N. Hunt, The turbulent transport of suspended sediment in open channels, Proc. R. Soc. Lond. Ser. A Math. Phys. Eng. Sci. 224 (1158) (1954) 322–335.
[46] Z. Cao, Equilibrium near-bed concentration of suspended sediment, J. Hydraul. Eng. 125 (12) (1999) 1270–1278.
[47] R.L. Soulsby, R.J.S. Whitehouse, Threshold of sediment motion in coastal environments, in: Proc. Comb. Aust. Coast. Eng. Port Conf, in: Cent. Adv. Eng., Univ. Canterbury, 1997, pp. 149–154.